Discontinuous Galerkin methods for Hyperbolic PDEs. Lecture 1

Olindo Zanotti
olindo.zanotti@unitn.it

University of Trento
Laboratory of Applied Mathematics

PiTP 2016
Computational Plasma Astrophysics
18 – 29 July 2016 - Princeton

www.exahype.eu

www.olindozanotti.net

Lecture 1

1. Basic terminology
2. A brief recap about numerical methods for Hyperbolic PDEs
3. Discontinuous Galerkin methods
   - A bit of history
   - The DG discretization
   - Polynomial basis
   - Non-linear L_2 stability
4. Runge–Kutta DG

Lecture 2

1. ADER Discontinuous Galerkin schemes
   - The ADER approach
   - The local-spacetime Discontinuous Galerkin predictor
   - Limiters for DG
2. Numerical tests
3. Tutorial session (Thursday afternoon)

Basic terminology

- Finite difference numerical methods evolve in time the point-values of the solution.
- Finite volume numerical methods evolve in time the cell averages of the solution.
- Discontinous Galerkin methods evolve in time the so-called degrees of freedom of the solution, i.e. the expansion coefficients with respect to given basis functions.

$$\mathbf{U}_h(\mathbf{x}, t) = \sum_{l=0}^{M} \psi_l(\mathbf{x}) \hat{\mathbf{U}}_l^n(t) = \psi_l(\mathbf{x}) \hat{\mathbf{U}}_l^n(t) \quad \mathbf{x} \in I_i \,,$$

In this course we illustrate the third methodology, but a basic understanding of finite volume methods is also needed and it will be summarized in the following.

A brief recap about numerical methods for Hyperbolic PDEs

Let us assume a system of PDE in conservative form as

$$\frac{\partial \mathbf{U}}{\partial t} + \nabla \cdot \mathbf{F}(\mathbf{U}) = 0, \qquad \mathbf{x} \in \Omega \subset \mathbb{R}^d, \quad t \in \mathbb{R}_0^+, \tag{1}$$

where $\mathbf{U}$ is the vector of so-called conserved quantities, while $\mathbf{F}(\mathbf{U}) = (\mathbf{f}, \mathbf{g}, \mathbf{h})$ is a non-linear flux tensor that depends on the state $\mathbf{U}$.
A system like (1) can always be written as

$$\partial_t \mathbf{U} + \mathbf{A} \cdot \nabla \mathbf{U} = 0\,, \tag{2}$$

where $\mathbf{A}(\mathbf{U}) = \partial \mathbf{F} / \partial \mathbf{U}$ is the Jacobian of the flux vector.

The system above is said to be *hyperbolic* if the matrix of coefficients $\mathbf{A}$ is diagonalisable with a set of real eigenvalues, or eigenspeeds, $\lambda_1, \ldots, \lambda_N$ and a corresponding set of N linearly independent *right eigenvectors* $\mathbf{R}^{(1)}, \ldots, \mathbf{R}^{(m)}$, such that $\mathbf{A}\mathbf{R}^{(i)} = \lambda_i \mathbf{R}^{(i)}$, $\Lambda = \mathbf{R}^{-1}\mathbf{A}\mathbf{R} = \mathrm{diag}(\lambda_1, \ldots, \lambda_N)$ is the diagonal matrix of eigenvalues and $\mathbf{R}$ the matrix of right eigenvectors.

- Hyperbolic PDEs in conservative form can be solved through **conservative numerical schemes**

$$\frac{\partial \mathbf{U}}{\partial t} + \nabla \cdot \mathbf{F}(\mathbf{U}) = \mathbf{S}$$

See
[Leveque, 1992], [LeVeque, 2002], [Martí and Müller, 2003], [Font, 2008], [Toro, 2009]

- Hyperbolic PDEs in non-conservative form require different approaches, like **path-conservative numerical schemes**

$$\partial_t \mathbf{U} + \mathbf{A} \cdot \nabla \mathbf{U} = \mathbf{S}$$

See
[Gallardo et al., 2007], [Castro et al., 2008], [Pares, 2006], [Dumbser et al., 2014], which are based on the theory proposed by [Maso et al., 1995]. A challenge for these methods is the generalization of Rankine-Hugoniot conditions for shock waves:

$$\mathbf{F}_L - \mathbf{F}_R = S(\mathbf{U}_L - \mathbf{U}_R)\,.$$

We will not cover this topic in our lectures.

Hyperbolic PDEs in physical sciences

There are good physical motivations to conjecture that all dynamic laws of physics at the macroscopic level can be written as a hyperbolic system, although such a formulation is not always available. Let us list the most prominent examples

- Classical [Leveque, 1992] and relativistic [Rezzolla and Zanotti, 2013] inviscid hydrodynamics
- Classical [Goedbloed and Poedts, 2004] and relativistic [Anile, 1990, Gammie et al., 2003] (ideal) magnetohydrodynamics
- Relativistic [Komissarov, 2007, Dumbser and Zanotti, 2009] (resistive) magnetohydrodynamics
- Relativistic irreversible thermodynamics [Israel, 1976, Del Zanna et al., 2013]
- Radiation hydrodynamics [Anile et al., 1992, Jiang et al., 2012]
- Linear elasticity [Käser and Dumbser, 2006]
- Hydrodynamical modeling of semiconductors [Anile and Muscato, 1995]
- Einstein equations [Reula, 1998, Alic et al., 2009]

The Finite Volume discretization

On each time-slice let use discretise the spatial domain into J computing cells $I_j = [x_{j-1/2}, x_{j+1/2}]$ of size $\Delta x = x_{j+1/2} - x_{j-1/2}$, with $j = 1, ..., J$. In addition, we define a spacetime control volume as $\Omega_j^{n+1/2} = I_j \times [t^n, t^{n+1}]$ and integrate Eq. (1) first in space over I_j

$$\frac{d}{dt} \int_{x_{j-1/2}}^{x_{j+1/2}} \mathbf{U}(x,t)dx = \mathbf{F}(\mathbf{U}(x_{j-1/2},t)) - \mathbf{F}(\mathbf{U}(x_{j+1/2},t)) \,, \tag{3}$$

and then in time between t^n and t^{n+1} to obtain

$$\begin{aligned} \int_{x_{j-1/2}}^{x_{j+1/2}} \mathbf{U}(x,t^{n+1})dx = & \int_{x_{j-1/2}}^{x_{j+1/2}} \mathbf{U}(x,t^n)dx \\ & + \int_{t^n}^{t^{n+1}} \mathbf{F}(\mathbf{U}(x_{j-1/2},t))dt - \int_{t^n}^{t^{n+1}} \mathbf{F}(\mathbf{U}(x_{j+1/2},t))dt \,. \end{aligned} \tag{4}$$

Equation (4) represents the integral form of the conservative equations (1).

We next define two new quantities, the *cell (volume) averages*

$$\mathbf{U}_j^n = \frac{1}{\Delta x}\int_{x_{j-1/2}}^{x_{j+1/2}} \mathbf{U}(x,t^n)dx\,, \tag{5}$$

and the *numerical fluxes*

$$\mathbf{F}_{j\pm 1/2} = \frac{1}{\Delta t}\int_{t^n}^{t^{n+1}} \mathbf{F}[\mathbf{U}(x_{j\pm 1/2},t)]dt\,, \tag{6}$$

such that (4) is rewritten as

$$\mathbf{U}_j^{n+1} = \mathbf{U}_j^n + \frac{\Delta t}{\Delta x}(\mathbf{F}_{j-1/2} - \mathbf{F}_{j+1/2})\,. \tag{7}$$

Because of the volume averages introduced in the definition (5), the numerical methods that **can be built** in this way are known as *finite-volume methods*.

Important remarks

$$\mathbf{U}_j^{n+1} = \mathbf{U}_j^n + \frac{\Delta t}{\Delta x}(\mathbf{F}_{j-1/2} - \mathbf{F}_{j+1/2})\,. \tag{8}$$

- This equation **does not (yet)** represent a numerical scheme and it is indeed exact as no mathematical approximation has been done yet.
- The exact *mathematical method* (8) becomes an approximate *numerical method* only when an approximation (and hence a truncation error) is introduced for the computation of the cell averages $\mathbf{U}_j$ and of the numerical fluxes $\mathbf{F}_{j\pm1/2}$.
- High Resolution Shock Capturing schemes (HRSC) are numerical schemes for conservation laws for which the computation of the numerical fluxes $\mathbf{F}_{j\pm1/2}$ in (8) is obtained through the solution of Riemann problems.
- Godunov method is the first order version of such schemes

The Riemann problem

From a mathematical point of view, the Riemann problem for a general nonlinear hyperbolic system is an initial-value problem with initial conditions given by

$$\mathbf{U}(x,0) = \begin{cases} \mathbf{U}_L & \text{if} \quad x < 0\,, \\ \\ \mathbf{U}_R & \text{if} \quad x > 0\,, \end{cases}$$

where $\mathbf{U}_L$ and $\mathbf{U}_R$ are two constant values, named "left" and "right" states, respectively.

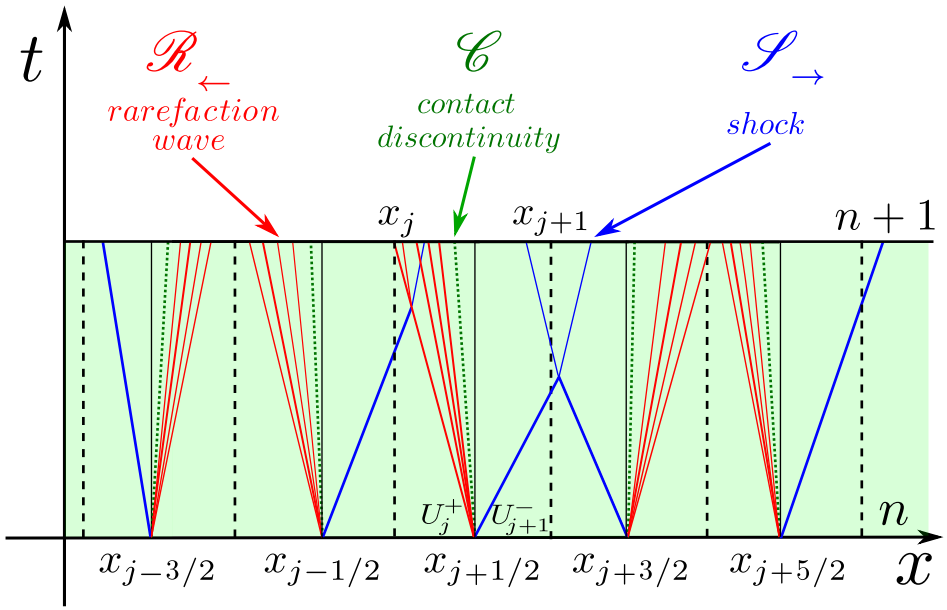

A numerical scheme is called a *conservative numerical scheme* if it is based on the conservation form of the PDEs. More specifically if

1. The numerical flux $\mathbf{F}_{j+1/2}$ (and analogously $\mathbf{F}_{j-1/2}$) depends on the values taken by $\mathbf{U}$ on the neighbouring cells, namely if

$$\mathbf{F}_{j+1/2} = \mathcal{F}(\mathbf{U}^n_{j-q}, \mathbf{U}^n_{j-q+1}, \ldots, \mathbf{U}^n_{j+r}), \tag{9}$$

   where q and r are integers and $\mathcal{F}$ is a numerical flux function of $q + r + 1$ arguments.

2. The flux function $\mathcal{F}$ reduces to the true physical flux in the case of constant flow, i.e. it satisfies the consistency condition

$$\mathcal{F}(\mathbf{U}, \ldots, \mathbf{U}) = \mathbf{F}(\mathbf{U}). \tag{10}$$

Note that the Riemann solver flux $\boldsymbol{F}_{j+1/2}$ is assumed to depend only on the values of $\boldsymbol{U}$ in the two adjacent cells, i.e. $r = 0 = q$ and

$$\boldsymbol{F}_{j+1/2} = \mathcal{F}(\boldsymbol{U}^n_j, \boldsymbol{U}^n_{j+1}). \tag{11}$$

Theorem *Conservative numerical schemes, if convergent, converge to the weak solution of the problem [Lax and Wendroff, 1960].*

Theorem *Non-conservative schemes do not converge to the correct solution if a shock wave is present in the flow [Hou and LeFloch, 1994].*

Briefly about weak solutions

Multiply the conservative form by a continuously differentiable function $\psi(x,t)$ of compact support, then integrate over space, with $x \in (-\infty, \infty)$, and time, with $t \in [0, \infty)$:

$$\int_0^{\infty} \int_{-\infty}^{+\infty} [\psi\, \partial_t \mathbf{U} + \psi\, \partial_x \mathbf{F}] dx\, dt = 0\,. \tag{12}$$

Integration by parts both in time and in space then leads to

$$\int_{-\infty}^{+\infty} \psi\, \mathbf{U} dx \Big|_{t=0}^{t=\infty} + \int_0^{\infty} \psi\, \mathbf{F} dt \Big|_{x=-\infty}^{x=+\infty} - \int_0^{\infty} \int_{-\infty}^{+\infty} \left[\mathbf{U}\, \partial_t \psi\, + \mathbf{F}\, \partial_x \psi\right]\, dx\, dt = 0\,, \tag{13}$$

and thus to

$$\int_0^{\infty} \int_{-\infty}^{+\infty} \left[\mathbf{U}\, \partial_t \psi\, + \mathbf{F}\, \partial_x \psi\right] dx\, dt = -\int_{-\infty}^{+\infty} \psi(x,0)\, \mathbf{U}(x,0)\, dx\,, \tag{14}$$

where we have used the property that ψ has compact support and therefore

$$\psi(x, t=\infty) = 0 = \psi(x=-\infty, t) = \psi(x=+\infty, t)\,. \tag{15}$$

A function $\mathbf{U}$ is then called a weak solution of the conservative equation if it satisfies the so-called weak formulation (14) for all functions ψ.

Godunov's first order method

In Godunov's first order method the left and right states of local Riemann problems are the **constant** cell averages.

$$\mathbf{U}(x,0) = \begin{cases} \mathbf{U}_j^n & \text{if} \quad x < x_{j+1/2}\,, \\ \\ \mathbf{U}_{j+1}^n & \text{if} \quad x > x_{j+1/2}\,. \end{cases} \tag{16}$$

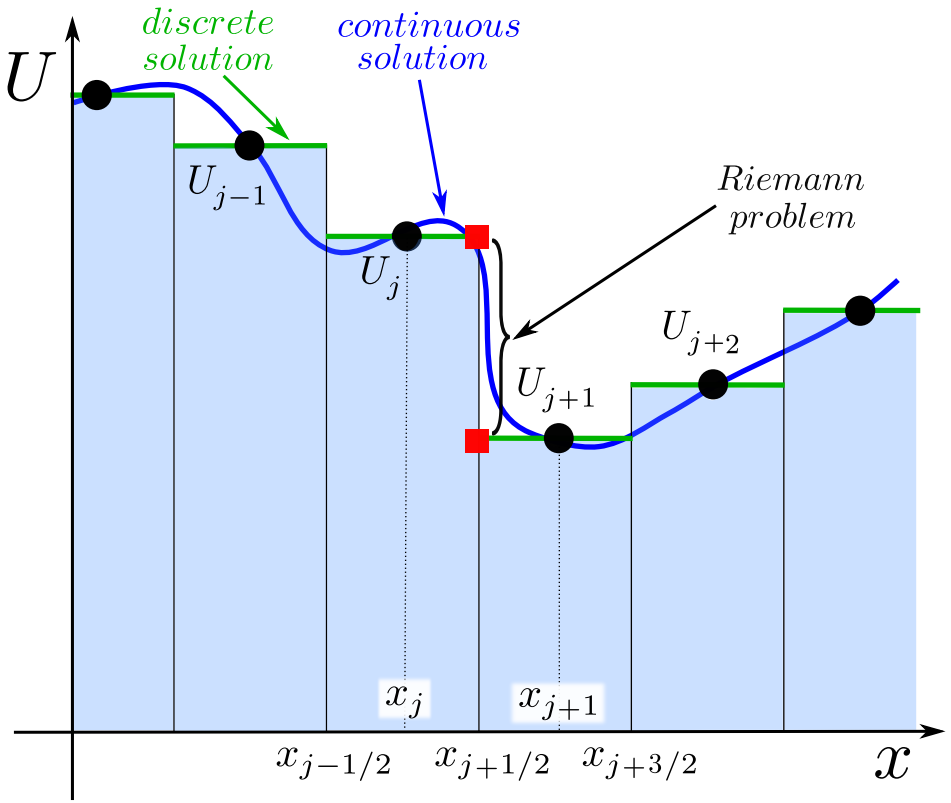

Going beyond first order

the local error E_j is the difference between the exact and the numerical solution at x_j^n, i.e.

$$E_j = |u_j - U_j| = C_1 \Delta x^{m_j} + C_2 \Delta t^{n_j} \tag{17}$$

- **Order of accuracy of a numerical scheme:** since $\Delta x \propto \Delta t$, we can define the order of accuracy as $p_j = \min(m_j, n_j)$.
- High order methods ($p_j \geq 2$) are preferred when the finest details of the solution are important.
- If a certain error is assumed to be acceptable, high order methods perform better than a lower order method over a highly refined mesh.
- Recall that in the presence of a discontinuity all methods deteriorate to first-order near the discontinuity.

However, there is Godunov theorem....

> ***Theorem*** *A linear (i.e. with constant coefficients) and monotonicity-preserving scheme is at most first-order accurate.*

- a method is said to be **monotonicity preserving** if

$$\mathbf{U}_j^n \geq \mathbf{U}_{j+1}^n \qquad \forall\, j\,, \tag{18}$$

  implies that

$$\mathbf{U}_j^{n+1} \geq \mathbf{U}_{j+1}^{n+1} \qquad \forall\, j\,. \tag{19}$$

  This property is crucial to prevent the appearance of oscillations.

- A scheme of the form

$$\mathbf{U}_j^{n+1} = \sum_{k=-l}^{k=r} b_k \mathbf{U}_{j+k}^n \tag{20}$$

  is **linear** if the b_k are constant.

Conclusion: high order schemes must be non-linear! (otherwise they will produce oscillations)

Example: Total Variation Diminishing (TVD) schemes

We can provide a piecewise-linear reconstruction of $\mathbf{U}_j(x)$ inside each cell

$$\mathbf{U}_j^n(x) = \mathbf{U}_j^n + \sigma_j^n(x - x_j) \qquad \text{with} \quad x_{j-1/2} \leq x \leq x_{x+j/2}\,, \tag{21}$$

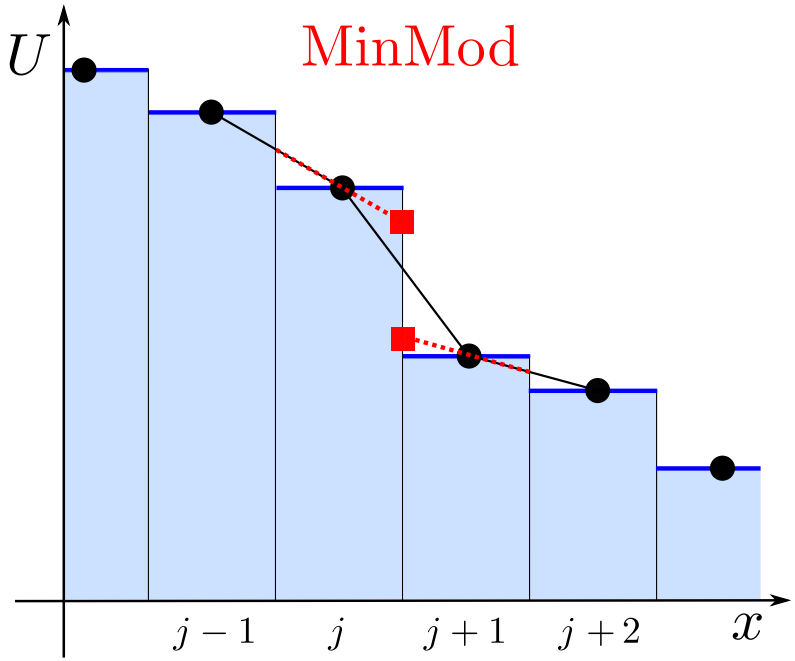

The non-linearity is hidden in the constant slope σ_j^n of the spatial reconstruction.

In the *minmod slope limiter* [Kolgan, 1972, van Leer, 1979]

$$\sigma_j^n = \text{minmod}\left(\frac{\mathbf{U}_j^n - \mathbf{U}_{j-1}^n}{\Delta x}, \frac{\mathbf{U}_{j+1}^n - \mathbf{U}_j^n}{\Delta x}\right), \tag{22}$$

$$\begin{aligned} \text{minmod}(\alpha,\beta) &= \begin{cases} \alpha & \text{if} \quad |\alpha| < |\beta| \text{ and} \quad \alpha\beta > 0\,, \\ \beta & \text{if} \quad |\beta| < |\alpha| \text{ and} \quad \alpha\beta > 0\,, \\ 0 & \text{if} \quad \alpha\beta \leq 0\,, \end{cases} \\ &= \text{sign}(\alpha)\,\text{max}\{0, \text{min}\{|\alpha|, \beta\,\text{sign}(\alpha)\}\}\,. \end{aligned} \tag{23}$$

Similarly, several non-linear schemes can be developed, ENO, WENO, etc., each of which providing a spatial reconstruction which depends on the solution itself, and is therefore non-linear.

Simple remark

Up to second order, finite difference (FD) and finite volume (FV) numerical schemes are essentially the same.

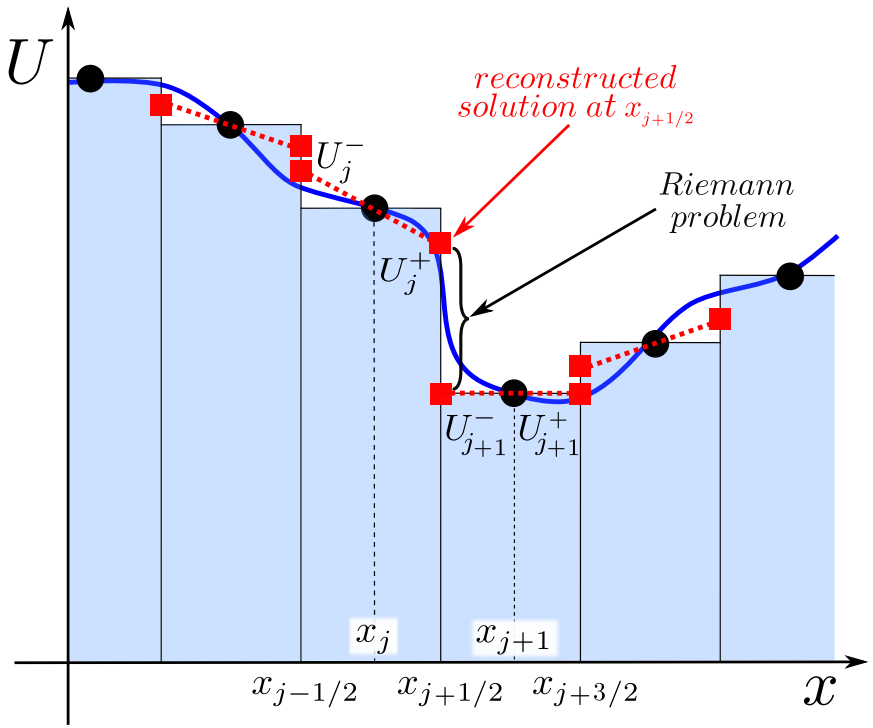

The method of lines

Eq. (7) can be regarded as an ODE

$$\begin{aligned}\frac{d\mathbf{U}_j(t)}{dt} &= \frac{1}{\Delta x}\left(\boldsymbol{F}[\boldsymbol{U}(x_{j-1/2},t)] - \boldsymbol{F}[\boldsymbol{U}(x_{j+1/2},t)]\right) + \boldsymbol{S}_j\,,\\ &=: \boldsymbol{L}(\mathbf{U}_j) + \boldsymbol{S}_j = Q(\mathbf{U}_j)\,,\end{aligned} \tag{24}$$

which can be solved through the multi-step **Runge–Kutta method** [Shu and Osher, 1988]. In general, starting from time $t = t^n$, the method consists in the computation of a number of predictor steps, indicated as $\mathbf{U}^{(i)}$ for the i-th substep, followed by the final update to time $t = t^{n+1}$,

$$\mathbf{U}^{(i)} = \sum_{k=0}^{i-1}\left(\alpha_{ik}\mathbf{U}^{(k)} + \Delta t\,\beta_{ik}\,Q(\mathbf{U}^{(k)})\right)\,, \qquad i = 1,\ldots,n+1\,, \tag{25}$$

$$\mathbf{U}^{(0)} = \mathbf{U}^n\,, \tag{26}$$

where α_{ik} and β_{ik} are constant coefficients.

Example: RK2

$$\begin{aligned} \mathbf{U}^{(1)} &= \mathbf{U}^n + \Delta t\, Q(\mathbf{U}^n)\,, \\ \mathbf{U}^{n+1} &= \frac{1}{2}\left[\mathbf{U}^n + \mathbf{U}^{(1)} + \Delta t\, Q(\mathbf{U}^{(1)})\right]\,, \end{aligned} \tag{27}$$

Example: RK3

$$\begin{aligned} \mathbf{U}^{(1)} &= \mathbf{U}^n + \Delta t\, Q(\mathbf{U}^n)\,, \\ \mathbf{U}^{(2)} &= \frac{1}{4}\left[3\mathbf{U}^n + \mathbf{U}^{(1)} + \Delta t\, Q(\mathbf{U}^{(1)})\right]\,, \\ \mathbf{U}^{n+1} &= \frac{1}{3}\mathbf{U}^n + \frac{2}{3}\mathbf{U}^{(2)} + \frac{2}{3}\Delta t\, Q(\mathbf{U}^{(2)})\,. \end{aligned} \tag{28}$$

There is also an implicit version (called IMEX Runge Kutta) that is used for stiff source terms.

The CFL condition

A first and *necessary* condition for stability is the so-called Courant–Friedrichs–Lewy (CFL) condition [Courant et al., 1967], which applies essentially to all explicit numerical schemes.

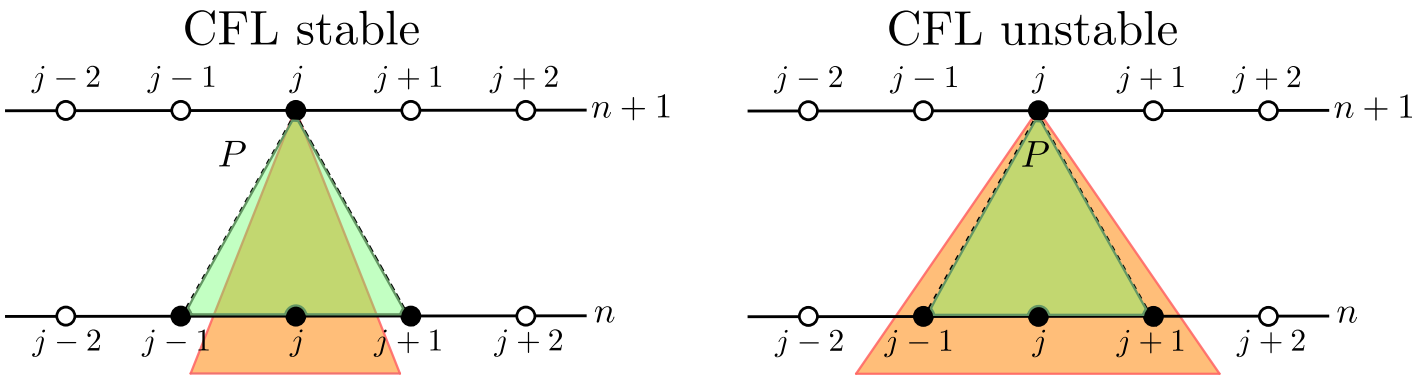

From a *physical* point of view the CFL condition ensures that the propagation speed of any physical perturbation is always smaller than the numerical speed defined as $\lambda_{\mathrm{N}} = \Delta x/\Delta t$, i.e.

$$|\lambda| \leq \lambda_{\mathrm{N}} = \frac{\Delta x}{\Delta t} \Longrightarrow \Delta t = c_{\mathrm{CFL}} \frac{\Delta x}{|\lambda|} \,. \tag{29}$$

Discontinuous Galerkin methods

A bit of history

- *Discontinuous Galerkin (DG) methods* can be considered as numerical methods for the weak formulation of the equations.
- They were first applied to first-order equations by [Reed and Hill, 1973],
- Their widespread use followed from the application to hyperbolic problems by Cockburn and collaborators in a series of articles [Cockburn and Shu, 1989, Cockburn et al., 1990, Cockburn, 1998].
- In the discontinuous Galerkin finite element framework the coefficients of higher order polynomials are directly evolved in time for each cell, **without the need of using a reconstruction operator**. This feature of DG schemes is in common with the classical finite element method (FEM).
- Unlike classical finite elements, the numerical solution given by a DG scheme is discontinuous at element interfaces and this discontinuity is resolved by the use of a numerical flux function, which is a common feature with HRSC finite volume schemes.
- Only relatively few implementations in the relativistic framework so far: [Zumbusch, 2009, Radice and Rezzolla, 2011, Zanotti et al., 2015, Teukolsky, 2016, Miller and Schnetter, 2016]

Pros:

- Once implemented, DG methods reach arbitrary order of accuracy in space by simply acting on the degree of the expansion polynomials
- They allow easily for hp-adaptation, i.e. they allow for refinement and recoarsening of the mesh and for a dynamical adaptation of the polynomial degree of the numerical solution.
- They incorporate Riemann solver, keeping the properties of upwind numerical schemes for conservation laws.
- Since they do not requires the introduction of reconstruction stencils, they typically require less MPI communications on parallel codes.
- They can be easily extended to general unstructured meshes
- Rubustness (DG methods are L_2 stable) and spectral convergence

Spectral convergence

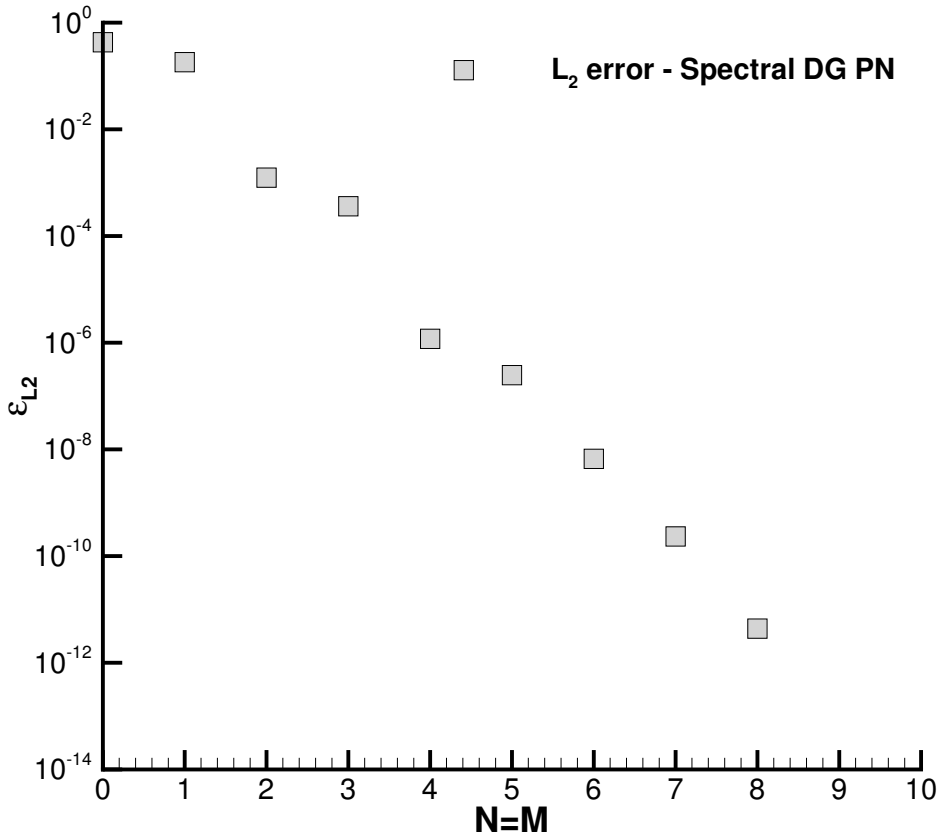

Contra:

- DG methods require a change of "philosophy" in the numerical schemes: we are no longer evolving in time point values nor cell averages.
- They are constrained by a more severe (w.r.t. finite volume) CFL condition.
- They require some special procedure to avoid oscillations at discontinuities.

The DG discretization

Assume a system of PDE in conservative form as

$$\frac{\partial \mathbf{U}}{\partial t} + \nabla \cdot \mathbf{F}(\mathbf{U}) = 0, \qquad \mathbf{x} \in \Omega \subset \mathbb{R}^d, \quad t \in \mathbb{R}_0^+, \tag{30}$$

where $\mathbf{U}$ is the vector of so-called conserved quantities, while $\mathbf{F}(\mathbf{U}) = (\mathbf{f}, \mathbf{g}, \mathbf{h})$ is a non-linear flux tensor that depends on the state $\mathbf{U}$. The computational domain Ω is discretized by a Cartesian grid composed by elements I_i, namely

$$\Omega = \bigcup_{i=1}^{N_E} I_i \,, \tag{31}$$

where the index i ranges from 1 to the total number of elements N_E. In the following, we denote the cell volume by $|I_i| = \int_{I_i} d\mathbf{x}$. At the beginning of each time-step, the numerical solution of Eq. (30) is represented within each cell I_i by piecewise polynomials of maximum degree $M \geq 0$ as

$$\mathbf{U}_h(\mathbf{x}, t^n) = \sum_{l=0}^{M} \psi_l(\mathbf{x}) \hat{\mathbf{U}}_l^n = \psi_l(\mathbf{x}) \hat{\mathbf{U}}_l^n \quad \mathbf{x} \in I_i \,, \tag{32}$$

where $\mathbf{U}_h$ is referred to as the *discrete representation* of the solution, while the coefficients $\hat{\mathbf{U}}_l^n$ are usually called the degrees of freedom.

We multiply Eq. (30) by a test function ψ_k, identical to the spatial basis functions of Eq. (32). Second, we integrate over the space element I_i.

$$\int_{I_i} \psi_k \frac{\partial \mathbf{U}_h}{\partial t} d\mathbf{x} + \int_{I_i} \psi_k \nabla \cdot \mathbf{F}(\mathbf{U}_h) \, d\mathbf{x} = 0 \,. \tag{33}$$

The flux divergence term is then integrated by parts in space, thus yielding

$$\int_{I_i} \psi_k \frac{\partial \mathbf{U}_h}{\partial t} d\mathbf{x} + \int_{\partial I_i} \psi_k \, \mathbf{F}(\mathbf{U}_h) \cdot \mathbf{n} \, dS - \int_{I_i} \nabla \psi_k \cdot \mathbf{F}(\mathbf{U}_h) \, d\mathbf{x} = 0, \tag{34}$$

where $\mathbf{n}$ is the outward pointing unit normal vector on the surface ∂I_i of element I_i. Since the discrete solution is allowed to be discontinuous at element boundaries, the surface integration involved in the second term of (34) is done through the solution of a Riemann problem, which is therefore deeply rooted in the DG scheme and guarantees the overall upwind character of the method [Cockburn and Shu, 1991].

CFL condition for DG schemes

Explicit DG schemes are limited by a Courant-Friedrichs-Lewy (CFL) restriction. There is not universal agreement about the most appropriate form of the time-step restriction. According to [Krivodonova and R.Qin, 2013] it is

$$\Delta t < \frac{1}{(2M+1)} \frac{h}{|\lambda_{\max}|}, \tag{35}$$

while, according to [Gottlieb and Tadmor, 1991, Radice and Rezzolla, 2011], it should be

$$\Delta t < \frac{1}{(M+1)^2} h \tag{36}$$

where h and $|\lambda_{\max}|$ are a characteristic mesh size and the maximum signal velocity, respectively.

First comments:

Although the constraint imposed by Eq. (35) may appear very severe and such as to make DG methods of little practical use, especially at high orders, this limitation is mitigated by two properties of DG methods.

- The first one is that discretisation with spacings much larger than those used in lower-order methods can be used with success.
- The second one is that local time-stepping can be performed, whereby each element is updated in time at its own maximum stable time-step, with a potential speedup that is progressively higher if only a small fraction of elements requires a small time-step (see [Hesthaven and Warburton, 2007] for details).

Polynomial basis

Modal (or hierarchical) basis

A modal, or hierarchical polynomial basis of maximum degree M, denoted as $\psi_k(\xi)$ here for convenience, is a set of $M+1$ linearly independent polynomials, with degree from zero to the maximum degree M. This is for instance the case of the orthogonal Legendre polynomials, which, rescaled on the reference element $E = [0, 1]$, are referred to as the shifted Legendre polynomials and are given by

$$
\begin{aligned}
\psi_0(\xi) &= 1\,, \\
\psi_1(\xi) &= 2\xi - 1\,, \\
\psi_2(\xi) &= 6\xi^2 - 6\xi + 1\,, \\
\psi_3(\xi) &= 20\xi^3 - 30\xi^2 + 12\xi - 1\,, \\
\psi_4(\xi) &= 70\xi^4 - 140\xi^3 + 90\xi^2 - 20\xi + 1\,, \\
\psi_5(\xi) &= 252\xi^5 - 630\xi^4 + 560\xi^3 - 210\xi^2 + 30\xi - 1\,, \\
&\vdots
\end{aligned}
\tag{37}
$$

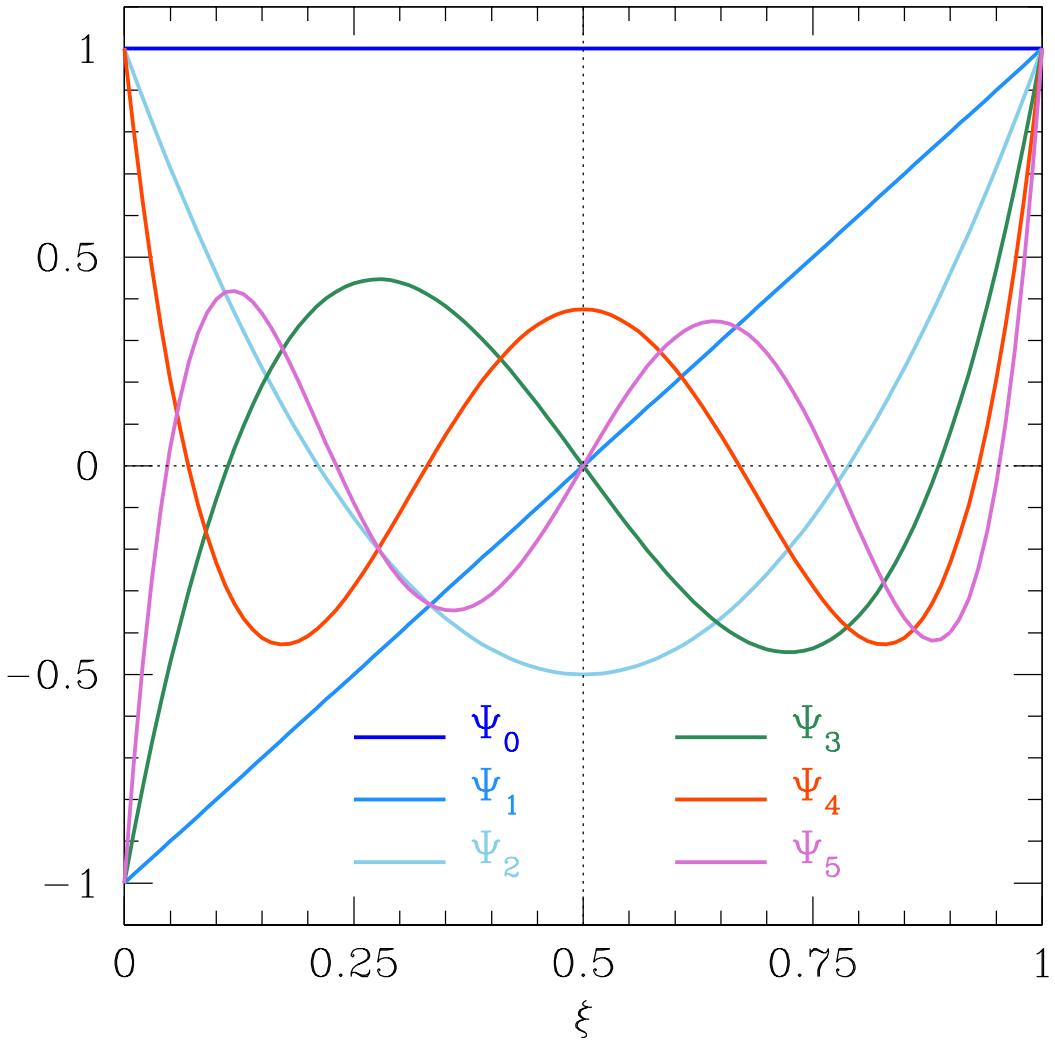

Figure : Functional behaviour of the first six shifted Legendre polynomials of a modal basis as given by expressions (37).

Nodal basis

A nodal basis of polynomials, all of degree M, is formed by $M+1$ such polynomials built in the following way [Solin, 2006]:

- We first consider a reference coordinate $\xi \in [0,1]$, defined by

$$x = x_{i-\frac{1}{2}} + \xi \Delta x_i, \tag{38}$$

- Compute the $M+1$ Gauss-Legendre quadrature nodes $\{\xi_k\}_{k=1}^{M+1}$ as the zeroes of the Legendre polynomials of order $M+1$.
- Compute the $M+1$ Lagrange interpolation polynomials, $\{\psi_l(\xi)\}_{l=1}^{M+1}$, passing through the $M+1$ Gauss-Legendre quadrature nodes $\{\xi_k\}_{k=1}^{M+1}$

$$\psi_l(\xi) = \prod_{n=1, n\neq l}^{M+1} \frac{\xi - \xi_n}{\xi_l - \xi_n} \tag{39}$$

- Note that

$$\psi_l(\xi_k) = \delta_{lk} \qquad l,k = 1,2,\ldots,M+1\,, \tag{40}$$

where δ_{lk} is the "Kronecker delta", i.e. $\delta_{lk} = 1$ if $l = k$, $\delta_{lk} = 0$ otherwise.

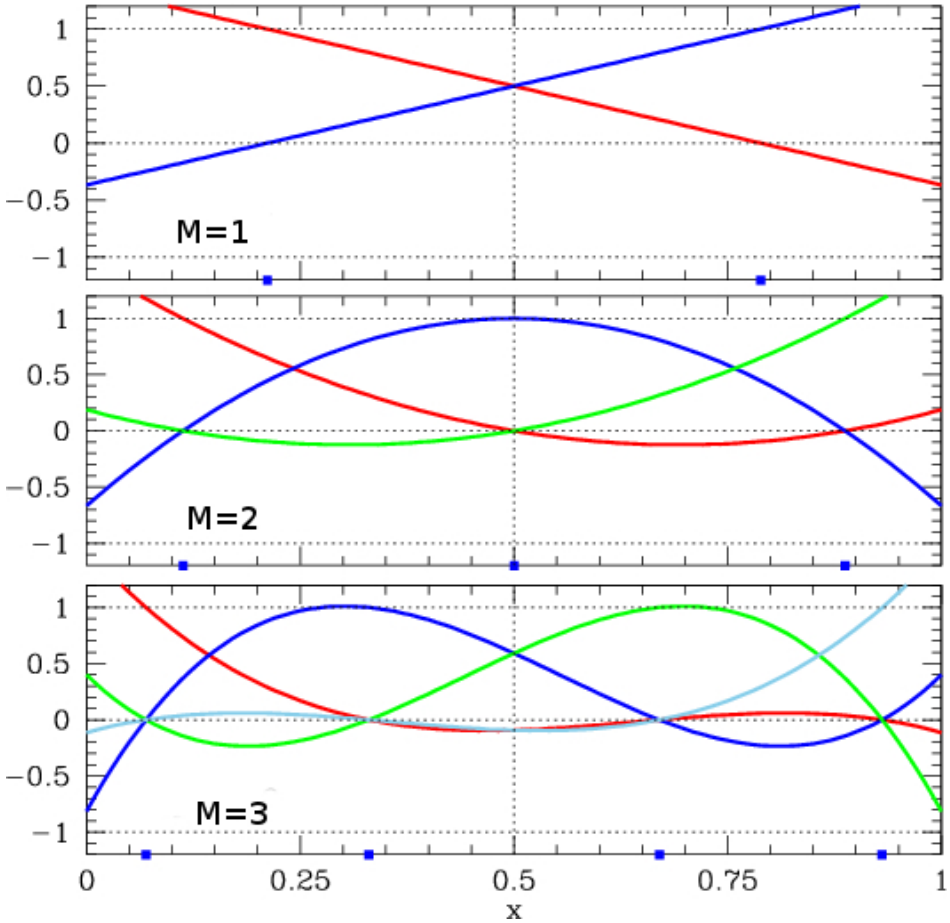

Figure : Functional form of the first polynomials of the nodal basis of degree M. The blue squares indicate the abscissas of the $M+1$ Gaussian points.

- In the programming practice, the computation of the $M+1$ Lagrange interpolation polynomials can be performed via solution of $M+1$ linear systems of the kind (example with $M=2$)

$$\begin{pmatrix} 1 & \xi_1 & \xi_1^2 \\ 1 & \xi_2 & \xi_2^2 \\ 1 & \xi_3 & \xi_3^2 \end{pmatrix} \begin{pmatrix} a \\ b \\ c \end{pmatrix} = \begin{pmatrix} 1 \\ 0 \\ 0 \end{pmatrix}$$

$$\begin{pmatrix} 1 & \xi_1 & \xi_1^2 \\ 1 & \xi_2 & \xi_2^2 \\ 1 & \xi_3 & \xi_3^2 \end{pmatrix} \begin{pmatrix} a' \\ b' \\ c' \end{pmatrix} = \begin{pmatrix} 0 \\ 1 \\ 0 \end{pmatrix}$$

$$\begin{pmatrix} 1 & \xi_1 & \xi_1^2 \\ 1 & \xi_2 & \xi_2^2 \\ 1 & \xi_3 & \xi_3^2 \end{pmatrix} \begin{pmatrix} a'' \\ b'' \\ c'' \end{pmatrix} = \begin{pmatrix} 0 \\ 0 \\ 1 \end{pmatrix}$$

Table : Coordinates of the Gauss–Legendre nodes and the corresponding nodal basis polynomials for a few values of M.

	ξ_k	ψ_l
$M = 1$		
	$\xi_1 = 0.2113248654051$	$\psi_1 = 1.366025403784 - 1.732050807568\xi$
	$\xi_2 = 0.7886751345948$	$\psi_2 = -0.3660254037844 + 1.732050807568\xi$
$M = 2$		
	$\xi_1 = 0.1127016653792$	$\psi_1 = 1.478830557701 - 4.624327782069\xi$ $+3.333333333333\xi^2$
	$\xi_2 = 0.5$	$\psi_2 = -0.6666666666666 + 6.666666666666\xi$ $-6.666666666666\xi^2$
	$\xi_3 = 0.8872983346207$	$\psi_3 = 0.1878361089654 - 2.042338884597\xi$ $+3.333333333333\xi^2$
$M = 3$		
	$\xi_1 = 6.9431844202973 \times 10^{-2}$	$\psi_1 = 1.526788125457 - 8.546023607872\xi$ $+14.32585835417\xi^2 - 7.42054006803894\xi^3$
	$\xi_2 = 0.3300094782075$	$\psi_2 = -0.8136324494869 + 13.80716692568\xi$ $-31.38822236344\xi^2 + 18.79544940755\xi^3$
	$\xi_3 = 0.6699905217924$	$\psi_3 = 0.4007615203116 - 7.417070421462\xi$ $+24.99812585921\xi^2 - 18.79544940755\xi^3$
	$\xi_4 = 0.9305681557970$	$\psi_4 = -0.1139171962819 + 2.155927103645\xi$ $-7.935761849944\xi^2 + 7.420540068038\xi^3$

- We also recall that, having selected the nodal points in this way, we will compute integrals through Gaussian quadrature rules

$$\int_0^1 g(\xi)d\xi \approx \sum_{k=1}^{M+1} \omega_k g(\xi_k) \tag{41}$$

and this integral is known to be exact for all polynomials up to degree $2\underbrace{(M+1)}_{\text{nodal points}} - 1 = 2M + 1$.

Non-linear L_2 stability

There is an important result due to [Jiang and Shu, 1994] who proved **a discrete cell entropy inequality for the square entropy** of the Discontinuous Galerkin scheme when applied to scalar nonlinear hyperbolic conservation laws.

Theorem *The Discontinuous Galerkin scheme is L_2 stable, i.e.*

$$\int_{\Omega} \partial_t \left(\frac{\mathrm{U}^2}{2} \right) dx \leq 0 \,. \tag{42}$$

- This property holds for arbitrary high order semi-discrete DG schemes and for any non-linear hyperbolic conservation law. The only requirements are that the space of the approximating solution and of the test functions are the same.
- This property makes DG schemes very robust (e.g. for strong vorticity problems), but it is not enough to prevent appearance of oscillations at shocks.

Proof of the theorem

We consider the scalar conservation law in the usual form

$$\partial_t \mathrm{U} + \partial_x \mathrm{f} = 0\,, \tag{43}$$

Definition
We define the square entropy and its associated flux (entropy flux) as

$$\mathcal{S}_2 = \frac{\mathrm{U}^2}{2} \qquad\qquad \mathcal{F}_2 = \mathrm{U}\ \mathrm{f}(\mathrm{U}) - \int f(\mathrm{U})\, d\mathrm{U} \tag{44}$$

Definition *A Lipschitz continuous function $\mathrm{f}_{i+1/2} = \mathrm{f}_{i+1/2}(\mathrm{U}^-, \mathrm{U}^+)$ of the two states U^- and U^+ is called an e-flux for the conservation law (43) if*

$$\mathrm{f}_{i+1/2}(\mathrm{U}, \mathrm{U}) = f(\mathrm{U})\,, \tag{45}$$

and

$$\int_{\mathrm{U}^-}^{\mathrm{U}^+} (f(\mathrm{U}) - \mathrm{f}_{i+1/2}(\mathrm{U}^-, \mathrm{U}^+))d\mathrm{U}\ \geq 0\,. \tag{46}$$

We assume that $\mathrm{U} \in V_h$ is an approximate solution of (43) in a discrete function space $V_h \subset L_2$.

$$L_2(\Omega) = \{g \in V : \left(\int_\Omega |g(x)|^2 dx \right)^{1/2} < \infty\}$$

We then multiply (43) by $\Phi \in V_h$ from the same function space and we integrate by parts, obtaining

$$\int_{I_i} \Phi \partial_t \mathrm{U} \, dx + (\mathrm{f}_{i+1/2} \Phi^-_{i+1/2} - \mathrm{f}_{i-1/2} \Phi^+_{i-1/2}) - \int_{I_i} \mathrm{f}(\mathrm{U}) \partial_x \Phi \, dx = 0 \,, \tag{47}$$

where $I_i = [x_{i-1/2}; x_{i+1/2}]$ is the cell size while

- $\mathrm{f}_{i-1/2} = \mathrm{f}_{i-1/2}(\mathrm{U}^-_{i-1/2}, \mathrm{U}^+_{i-1/2})$ is an e-flux between I_{i-1} and I_i.
- $\mathrm{f}_{i+1/2} = \mathrm{f}_{i+1/2}(\mathrm{U}^-_{i+1/2}, \mathrm{U}^+_{i+1/2})$ is an e-flux between I_i and I_{i+1}.
- $\Phi^-_{i+1/2} = \Phi(x^-_{i+1/2})$ and $\Phi^+_{i-1/2} = \Phi(x^+_{i-1/2})$

Theorem *The numerical solution* $\mathrm{U} \in V_h$ *of the Discontinuous Galerkin scheme* (47) *(in which* $\mathrm{f}_{i\pm 1/2}$ *is an e-flux) obeys the discrete cell-entropy condition*

$$\int_{I_i} \partial_t \left(\frac{\mathrm{U}^2}{2} \right) dx + \hat{F}_{i+1/2} - \hat{F}_{i-1/2} \leq 0 \,. \tag{48}$$

Proof

Since both U and Φ belong to V_h, we can replace Φ with U in (47), to find

$$\int_{I_i} \partial_t \left(\frac{\mathrm{U}^2}{2} \right) dx + (\mathrm{f}_{i+1/2} \mathrm{U}^-_{i+1/2} - \mathrm{f}_{i-1/2} \mathrm{U}^+_{i-1/2}) - \int_{I_i} \mathrm{f}(\mathrm{U}) \partial_x \mathrm{U} \, dx = 0 \,. \tag{49}$$

We now rewrite the last term as

$$\int_{I_i} \mathrm{f}(\mathrm{U}) \partial_x \mathrm{U} \, dx = \int_{\mathrm{U}^+_{i-1/2}}^{\mathrm{U}^-_{i+1/2}} \mathrm{f}(\mathrm{U}) d\,\mathrm{U} = g(\mathrm{U}^-_{i+1/2}) - g(\mathrm{U}^+_{i-1/2}) \tag{50}$$

with the definition

$$g = \int \mathrm{f}(\mathrm{U}) d\,\mathrm{U} \,. \tag{51}$$

Therefore, (49) takes the form

$$\int_{I_i} \partial_t \left(\frac{\mathrm{U}^2}{2} \right) dx + (\mathrm{f}_{i+1/2}\mathrm{U}^-_{i+1/2} - g(\mathrm{U}^-_{i+1/2})) - (\mathrm{f}_{i-1/2}\mathrm{U}^+_{i-1/2} - g(\mathrm{U}^+_{i-1/2})) = 0\,, \tag{52}$$

which we can also rewrite as

$$\begin{aligned} \int_{I_i} \partial_t \left(\frac{\mathrm{U}^2}{2} \right) dx \quad &+ \quad (\mathrm{f}_{i+1/2}\mathrm{U}^-_{i+1/2} - g(\mathrm{U}^-_{i+1/2})) - (\mathrm{f}_{i-1/2}\mathrm{U}^-_{i-1/2} - g(\mathrm{U}^-_{i-1/2})) \\ &- \quad (\mathrm{f}_{i-1/2}\mathrm{U}^+_{i-1/2} - g(\mathrm{U}^+_{i-1/2})) + (\mathrm{f}_{i-1/2}\mathrm{U}^-_{i-1/2} - g(\mathrm{U}^-_{i-1/2})) \\ \int_{I_i} \partial_t \left(\frac{\mathrm{U}^2}{2} \right) dx \quad &+ \quad \hat{F}_{i+1/2} - \hat{F}_{i-1/2} + \hat{R}_{i-1/2} = 0\,, \end{aligned} \tag{53}$$

where

$$\hat{F}_{i+1/2} = (\mathrm{f}_{i+1/2}\mathrm{U}^-_{i+1/2} - g(\mathrm{U}^-_{i+1/2})) \tag{54}$$

$$\hat{F}_{i-1/2} = (\mathrm{f}_{i-1/2}\mathrm{U}^-_{i-1/2} - g(\mathrm{U}^-_{i-1/2})) \tag{55}$$

$$\hat{R}_{i-1/2} = -(\mathrm{f}_{i-1/2}\mathrm{U}^+_{i-1/2} - g(\mathrm{U}^+_{i-1/2})) + (\mathrm{f}_{i-1/2}\mathrm{U}^-_{i-1/2} - g(\mathrm{U}^-_{i-1/2})) \tag{56}$$

We now notice that the terms $\hat{F}_{i+1/2}$ and $\hat{F}_{i-1/2}$ are discrete entropy fluxes consistent with the continuous entropy flux of Eq. (44). The term $\hat{R}_{i-1/2}$ can be written more coincisely as

$$\hat{R}_{i-1/2} = \int_{\mathrm{U}^-_{i-1/2}}^{\mathrm{U}^+_{i-1/2}} \left(\mathrm{f}(\mathrm{U}) - \mathrm{f}_{i-1/2}(\mathrm{U}^-_{i-1/2}, \mathrm{U}^+_{i-1/2}) \right) \, d\mathrm{U} \tag{57}$$

Due to the property (46), we know that $\hat{R}_{i-1/2} \geq 0$, and therefore, from (53) it follows that

$$\int_{I_i} \partial_t \left(\frac{\mathrm{U}^2}{2} \right) \, dx + \hat{F}_{i+1/2} - \hat{F}_{i-1/2} \leq 0 \, . \tag{58}$$

Corollary *The Discontinuous Galerkin scheme* (47) *is* L_2 *stable.*

In fact, summing (58) over all elements I_i and imposing either periodic boundary conditions or zero fluxes at the borders of the domain Ω we get

$$\int_{\Omega} \partial_t \left(\frac{\mathrm{U}^2}{2} \right) \, dx \leq 0 \, . \tag{59}$$

- The amount of numerical dissipation introduced is controlled by the term $\hat{R}_{i-1/2}$, which is always positive and it is related to the jump in U. The dissipation increases when the jump increases.

Runge–Kutta DG

Substituting $\mathbf{U}_h(\mathbf{x},t) = \psi_l(\mathbf{x})\hat{\mathbf{U}}_l^n(t)$ into

$$\int_{I_i} \psi_k \frac{\partial \mathbf{U}_h}{\partial t}\, d\mathbf{x} + \int_{\partial I_i} \psi_k\, \mathbf{F}\left(\mathbf{U}_h\right)\cdot \mathbf{n}\, dS - \int_{I_i} \nabla\psi_k \cdot \mathbf{F}\left(\mathbf{U}_h\right) d\mathbf{x} = 0,$$

yields the expression (think about 1D for the moment)

$$\sum_{l=0}^{M}\left(\int_0^1 \psi_l\psi_k\, d\xi\right)\frac{d\hat{\mathbf{U}}_l}{dt} + \left[\psi_k \mathbf{F}^*\right]_0^1 - \int_0^1 \mathbf{F}^*(\mathbf{U}(\xi,t))\frac{d\psi_k}{d\xi}\, d\xi = 0\ , \qquad (60)$$

which represents a system of (coupled) ordinary differential equations in time for the degrees of freedom $\hat{\mathbf{U}}_l(t)$. The advantage of this procedure is that the basis functions ψ_l are known analytically, so that also their derivatives, $\frac{d\psi_k}{d\xi}$, are also known analytically. As a result, the integral in the first term in (60) is analytic and needs to be calculated only once.

Example: let us consider the case of a fourth-order representation, namely with $M = 3$, of the function $\mathbf{U}(\xi,t)$. In this case it is more instructive to adopt a modal basis. We write

$$\mathbf{U}(\xi,t) = \hat{\mathbf{U}}_0(t)\psi_0(\xi) + \hat{\mathbf{U}}_1(t)\psi_1(\xi) + \hat{\mathbf{U}}_2(t)\psi_2(\xi) + \hat{\mathbf{U}}_3(t)\psi_3(\xi)\,. \qquad (61)$$

The corresponding system of (coupled) ordinary differential equations obtained from (60) is

$$\frac{d\hat{\mathbf{U}}_0}{dt} + \mathbf{F}^*(1) - \mathbf{F}^*(0) = 0\,, \tag{62}$$

$$\frac{1}{3} \quad \frac{d\hat{\mathbf{U}}_1}{dt} + \psi_1(1)\mathbf{F}^*(1) - \psi_1(0)\mathbf{F}^*(0) - \int_0^1 \mathbf{F}^*(\mathbf{U}(\xi,t))\,\frac{d\psi_1}{d\xi}\,d\xi = 0\,, \tag{63}$$

$$\frac{1}{5} \quad \frac{d\hat{\mathbf{U}}_2}{dt} + \psi_2(1)\mathbf{F}^*(1) - \psi_2(0)\mathbf{F}^*(0) - \int_0^1 \mathbf{F}^*(\mathbf{U}(\xi,t))\,\frac{d\psi_2}{d\xi}\,d\xi = 0\,, \tag{64}$$

$$\frac{1}{7} \quad \frac{d\hat{\mathbf{U}}_3}{dt} + \psi_3(1)\mathbf{F}^*(1) - \psi_3(0)\mathbf{F}^*(0) - \int_0^1 \mathbf{F}^*(\mathbf{U}(\xi,t))\,\frac{d\psi_3}{d\xi}\,d\xi = 0\,, \tag{65}$$

and can be solved through a standard Runge–Kutta discretisation in time, leading to a *Runge–Kutta discontinuous Galerkin scheme* [Balsara et al., 2007].

Comments

- To first order, namely when considering only Eq. (62), the RKDG scheme coincides with a first-order finite-volume scheme.
- The values of the fluxes at the cell borders, $\mathbf{F}^*(0)$ and $\mathbf{F}^*(1)$, can be obtained by solving a Riemann problem, thus incorporating the upwind property into the RKDG scheme.
- At least in principle, the solution of such Riemann problems does not require any spatial reconstruction at the interface between adjacent cells. The value of $\mathbf{U}$ at the cell borders is in fact naturally provided by the expansion (32) computed at the proper locations. However, if the discontinuities are strong, the scheme generates significant oscillations.
- The majority of DG schemes, including the astrophysical context, are in fact RKDG schemes.
- The efficiency of RK time discretization decreases if the order of accuracy is higher than four: the number of intermediate stages becomes larger than the formal order of accuracy, the so called "Butcher barrier".

References I

Alic, D., Bona, C., and Bona-Casas, C. (2009).
Towards a gauge-polyvalent numerical relativity code.
Phys. Rev. D, 79(4):044026.

Anile, A., Pennisi, S., and Sammartino, M. (1992).
Covariant radiation hydrodynamics.
Ann. Inst. Henri Poincaré, Phys. Théor., 56(1):49–74.

Anile, A. M. (1990).
Relativistic Fluids and Magneto-fluids.
Cambridge University Press.

Anile, A. M. and Muscato, O. (1995).
Improved hydrodynamical model for carrier transport in semiconductors.
Phys. Rev. B, 51:16728–16740.

Balsara, D. S., Altmann, C., Munz, C., and Dumbser, M. (2007).
A sub-cell based indicator for troubled zones in RKDG schemes and a novel class of hybrid RKDG+HWENO schemes.
Journal of Computational Physics, 226:586–620.

Castro, M., Gallardo, J., López, J., and Parés, C. (2008).
Well-balanced high order extensions of godunov's method for semilinear balance laws.
SIAM Journal of Numerical Analysis, 46:1012–1039.

Cockburn, B. (1998).
The Runge Kutta Discontinuous Galerkin Method for Conservation Laws V Multidimensional Systems.
Journal of Computational Physics, 141:199–224.

References II

Cockburn, B., How, S., and Shu, C. (1990).

TVB Runge Kutta Local Projection Discontinuous Galerkin Finite Element Method for Conservation Laws IV: The Multidimensional Case.
Math. Comp., 54:545.

Cockburn, B. and Shu, C. (1989).

TVB Runge Kutta Local Projection Discontinuous Galerkin Finite Element Method for Scalar Conservation Laws II: General Framework.
Math. Comp., 52:411.

Cockburn, B. and Shu, C. W. (1991).

The Runge-Kutta local projection P1-Discontinuous Galerkin finite element method for scalar conservation laws.
Mathematical Modelling and Numerical Analysis, 25:337–361.

Courant, R., Friedrichs, K., and Lewy, H. (1967).

On the Partial Difference Equations of Mathematical Physics.
IBM Journal of Research and Development, 11:215–234.

Del Zanna, L., Chandra, V., Inghirami, G., Rolando, V., Beraudo, A., De Pace, A., Pagliara, G., Drago, A., and Becattini, F. (2013).

Relativistic viscous hydrodynamics for heavy-ion collisions with ECHO-QGP.
European Physical Journal C, 73:2524.

Dumbser, M., Hidalgo, A., and Zanotti, O. (2014).

High Order Space-Time Adaptive ADER-WENO Finite Volume Schemes for Non-Conservative Hyperbolic Systems.
Computer Methods in Applied Mechanics and Engineering, 268:359–387.

References III

Dumbser, M. and Zanotti, O. (2009).
Very high order PNPM schemes on unstructured meshes for the resistive relativistic MHD equations.
Journal of Computational Physics, 228:6991–7006.

Font, J. A. (2008).
Numerical hydrodynamics and magnetohydrodynamics in general relativity.
Living Rev. Relativ., 6:4; http://www.livingreviews.org/lrr–2008–7.

Gallardo, J., Parés, C., and Castro, M. (2007).
On a well-balanced high-order finite volume scheme for shallow water equations with topography and dry areas.
Journal of Computational Physics, 227:574–601.

Gammie, C. F., McKinney, J. C., and Tóth, G. (2003).
Harm: A numerical scheme for general relativistic magnetohydrodynamics.
Astrophys. J., 589:458.

Goedbloed, J. P. H. and Poedts, S. (2004).
Principles of Magnetohydrodynamics.

Gottlieb, D. and Tadmor, E. (1991).
The CFL condition for spectral approximations to hyperbolic initial-boundary value problems.
Mathematics of Computation, 56(194):565–588.

Hesthaven, J. and Warburton, T. (2007).
Nodal Discontinuous Galerkin Methods: Algorithms, Analysis, and Applications.
Texts in Applied Mathematics. Springer.

References IV

Hou, T. Y. and LeFloch, P. G. (1994).
Why Nonconservative Schemes Converge to Wrong Solutions: Error Analysis.
Math. Comp., 62:497–530.

Israel, W. (1976).
Nonstationary irreversible thermodynamics: A causal relativistic theory.
Annals of Physics, 100:310–331.

Jiang, G. S. and Shu, C.-W. (1994).
On a cell entropy inequality for discontinuous Galerkin methods.
Mathematics of Computation, 62:531–538.

Jiang, Y.-F., Stone, J. M., and Davis, S. W. (2012).
A Godunov Method for Multidimensional Radiation Magnetohydrodynamics Based on a Variable Eddington Tensor.
Astrophysical Journal Suppl. Series, 199:14.

Käser, M. and Dumbser, M. (2006).
An arbitrary high-order discontinuous Galerkin method for elastic waves on unstructured meshes - I. The two-dimensional isotropic case with external source terms.
Geophysical Journal International, 166:855–877.

Kolgan, V. P. (1972).
Application of the minimum-derivative principle in the construction of finite-difference schemes for numerical analysis of discontinuous solutions in gas dynamics.
Transactions of the Central Aerohydrodynamics Institute, 3(6):68–77.
in Russian.

References V

Komissarov, S. S. (2007).
Multidimensional numerical scheme for resistive relativistic magnetohydrodynamics.
Mon. Not. R. Astron. Soc., 382:995–1004.

Krivodonova, L. and R.Qin (2013).
An analysis of the spectrum of the discontinuous galerkin method.
Applied Numerical Mathematics, 64:1–18.

Lax, P. D. and Wendroff, B. (1960).
Systems of conservation laws.
Commun. Pure Appl. Math., 13:217–237.

Leveque, R. J. (1992).
Numerical Methods for Conservation Laws.
Birkhauser Verlag, Basel.

LeVeque, R. J. (2002).
Finite Volume Methods for Hyperbolic Problems.
Cambridge University Press.

Martí, J. M. and Müller, E. (2003).
Numerical hydrodynamics in special relativity.
Living Rev. Relativ., 6:7; http://www.livingreviews.org/lrr–2003–7.

Maso, G. D., LeFloch, P., and Murat, F. (1995).
Definition and weak stability of nonconservative products.
J. Math. Pures Appl., 74:483–548.

References VI

Miller, J. M. and Schnetter, E. (2016).

An Operator-Based Local Discontinuous Galerkin Method Compatible With the BSSN Formulation of the Einstein Equations.
ArXiv e-prints.

Pares, C. (2006).

Numerical methods for nonconservative hyperbolic systems: a theoretical framework.
SIAM J. Numer. Anal., 44(1):300–321.

Radice, D. and Rezzolla, L. (2011).

Discontinuous Galerkin methods for general-relativistic hydrodynamics: Formulation and application to spherically symmetric spacetimes.
Phys. Rev. D, 84(2):024010.

Reed, W. H. and Hill, T. R. (1973).

Triangular mesh methods for the neutron transport equation.
Technical report, Los Alamos Scientific Laboratory.

Reula, O. (1998).

Hyperbolic methods for Einstein's equations.
Living Rev. Relativ., 1:3.

Rezzolla, L. and Zanotti, O. (2013).

Relativistic Hydrodynamics.
Oxford University Press, Oxford UK.

References VII

Shu, C. W. and Osher, S. J. (1988).

Efficient implementation of essentially non-oscillatory shock-capturing schemes.
J. Comput. Phys., 77:439.

Solin, P. (2006).

Partial Differential Equations And the Finite Element Method.
Pure and Applied Mathematics. Wiley-Interscience.

Teukolsky, S. A. (2016).

Formulation of discontinuous Galerkin methods for relativistic astrophysics.
Journal of Computational Physics, 312:333–356.

Toro, E. F. (2009).

Riemann Solvers and Numerical Methods for Fluid Dynamics.
Springer-Verlag.

van Leer, B. (1979).

Towards the ultimate conservative difference scheme. v. a second-order sequel to godunov's method.
Journal of Computational Physics, 32(1):101 – 136.

Zanotti, O., Fambri, F., and Dumbser, M. (2015).

Solving the relativistic magnetohydrodynamics equations with ADER discontinuous Galerkin methods, a posteriori subcell limiting and adaptive mesh refinement.
Mon. Not. R. Astron. Soc., 452:3010–3029.

Zumbusch, G. (2009).

Finite element, discontinuous Galerkin, and finite difference evolution schemes in spacetime.
Classical Quantum Gravity, 26(17):175011.